Differentiation of Vulnerable Carotid Plaques by Analysis of Calcium Content and Spectral Curve Slope using Gemstone Spectral Imaging

Ze-Xin Fan
Capital Medical University
Xiao-Qing Li
Capital Medical University
Ting-Ting Yang
Capital Medical University
Shao-Jie Yuan
Second Hospital of Shanxi Medical University
Tian-Tong Niu
Capital Medical University
Lin Ma
Capital Medical University
Kai Sun
Second Hospital of Shanxi Medical University
Li Wang
Second Hospital of Shanxi Medical University
Guang-Zhi Liu (guangzhi2002@hotmail.com)
Capital Medical University

Research Article

Keywords: plaque vulnerability, gemstone spectral imaging, high-sensitivity C-reactive protein, monocyte chemotactic protein-1, calcium content, spectral curve slope

Posted Date: May 17th, 2021

DOI: https://doi.org/10.21203/rs.3.rs-515069/v1

Abstract

Growing evidence indicates that vulnerable carotid plaque rupture is an important cause of stroke. However, fewer studies have been conducted to investigate the role of a novel gemstone spectral imaging (GSI) in assessment of vulnerable carotid plaque. In this study, we analyzed GSI data including calcium content of carotid atherosclerotic plaque and spectral curve slope, as well as serum high-sensitivity C-reactive protein (Hs-CRP), monocyte chemotactic protein-1 (MCP-1) levels in patients with carotid atherosclerotic plaque using the GSI-computed tomographic angiography (CTA) and immunoturbidimetry. The patients with unstable plaques demonstrated a significantly lower calcium content and higher spectral curve slope than the stable plaques group. In addition, the patients with unstable plaque showed an increase in Hs-CRP levels and MCP-1 levels compared with the stable plaque and normal controls (NC) group. The alternation in GSI calcium content and spectral curve slope reflects a close link between calcification and plaque instability, while derangement of Hs-CRP and MCP-1 is involved in the formation or development of vulnerable plaques. Taken together, our results strongly support the feasibility of using these serological and newly discovered imaging parameters as multiple potential biomarkers relevant to plaque vulnerability or stroke progression.

Introduction

Atherosclerosis is a lipid-driven chronic disease that leads to plaque formation in the arterial wall through intimal inflammation, necrosis, fibrosis and calcification [1–3]. As one of the critical factors of ischemic stroke [4, 5], atherosclerotic carotid plaque contains lipid-rich necrotic core (LRNC), intraplaque hemorrhage (IPH), calcification, and fibrous components, and vulnerable carotid plaque tends to consist of LRNC and IPH, rather than calcification and fibrous components [6, 7]. Of note, growing evidence indicates that vulnerable plaque rupture, instead of perfusion defects caused by luminal stenosis, is an important cause of stroke [5, 8–10]. Hence, in designing therapeutic intervention for effective stroke prevention, it is crucial to identify carotid atherosclerotic plaque and high-risk determinants as early as possible. So far, various plaque imaging (e.g., ultrasound, CT, and MRI) and serologic biomarkers of vulnerability (e.g., high-sensitivity C-reactive protein (Hs-CRP), matrix metalloproteinase (MMP)-9, sCD40 ligand (sCD40L)) have been adopted to predict the risk of cerebrovascular events [11].

Among these neuroimaging technologies, a novel gemstone spectral imaging (GSI) that incorporates computed tomographic angiography (CTA) with a gemstone detector, received increasing attention in recent years, as it allow for both monochromatic energy imaging and material basis decomposition. More importantly, GSI holds great potential to better characterize and quantify the concentration of the plaque components such as lipid, calcification and fibrous tissue [12], so as to accurately distinguish vulnerable plaques from stable plaques in carotid arteries. However, fewer studies have been conducted to investigate the role of GSI in assessment of vulnerable carotid plaque. In a recent study comparing the applicability of GSI to that of 3-dimensional time of-flight magnetic resonance angiography (MRA) in patients with carotid artery stenosis, Shinohara, et al. reported that effective Z value of noncalcified carotid plaques was remarkably lower in the group with high signal intensity than in the group with low

signal intensity on MRA, indicating utilization potential of GSI for identification of vulnerable carotid plaque [13]. Nevertheless, there is still a pressing need for further studies of a comprehensive evaluation of carotid atherosclerotic plaque using both imaging biomarkers and serological biomarkers as well as their possible roles in the atherogenetic process. Therefore, we have analyzed GSI-CTA data and serum Hs-CRP, monocyte chemotactic protein-1 (MCP-1) levels in patients with this disease to address these issues.

Results

Basic characteristics

Patients' characteristics including risk factors and laboratory data taken on the first day of sampling are shown in Table 1. No significant differences were found between NC and either of the carotid atherosclerosis groups.

Table 1
Baseline characteristics of patients and normal controls(NC)

	Unstable plaque (n = 17)	Stable plaque (n = 25)	NC (n = 19)	P value
Age (year)	63.29 ± 11.91	63.80 ± 9.57	60.32 ± 11.84	0.555
Female (%)	12 (70.59%)	15 (60.00%)	10 (52.63%)	0.543
Diabetes (%)	3 (17.65%)	5 (20.00%)	2 (10.52%)	0.693
Coronary artery disease (%)	3 (17.65%)	2(8.00%)	2(10.52%)	0.621
Dyslipidemia (%)	10 (58.82%)	9 (36.00%)	4 (21.05%)	0.064
Hypertension (%)	7 (41.18%)	9 (36.00%)	4 (21.05%)	0.397
Smoking (%)	7 (41.18%)	7 (41.18%)	4 (21.05%)	0.665
Peripheral artery disease (%)	7 (41.18%)	8 (32.00%)	4 (21.05%)	0.426
Leukocyte ($\times 10^3/\mu l$)	7.01 ± 2.12	7.06 ± 1.65	6.86 ± 1.92	0.935
Carotid stenosis (%) > 50% ≤ 50%	6 (35.29%) 11 (64.71%)	11 (44.00%) 14 (56.00%)		0.318
monocyte ($\times 10^3/\mu l$)	0.39 ± 0.11	0.38 ± 0.09	0.35 ± 0.10	0.450

Carotid atherosclerotic plaque characterization by GSI

Of the 42 patients with carotid atherosclerosis, 17 cases had unstable plaque (including 11 lipid cores plaques and 11 fibrous plaques) and 25 cases had stable plaque (including 30 calcified plaques). In the unstable plaque group, the position of atherosclerosis plaque was common carotid artery bifurcation (12/22, 54.5%), common carotid artery (5/22, 22.7%), external carotid artery (5/22, 22.7%), respectively. In the stable plaque group, there were 15 cases with common carotid artery bifurcation (15/30, 50%), 8 cases with common carotid artery (8/30, 26.7%) and 7 cases with external carotid artery (7/30, 23.3%).

Calcium content in plaques and slope of spectral curve by GSI

In the selected ROI area, the calcium content was significantly lower in unstable plaque group (47.53 ± 37.17 g/L) than the stable plaque group (147.85 ± 49.54 g/L, $P < 0.001$), while the slope of spectral curve was remarkably higher in unstable plaques group [0.29 (-3.86, 3.00)] than the stable plaque group [-6.55 (-14.55, -4.50), $P < 0.001$] (Fig. 2).

Serum Hs-CRP and MCP-1 levels

Patients with unstable plaques showed an increased Hs-CRP levels (14.74 ± 4.91 mg/L) compared with the stable and NC groups (2.65 ± 1.62 mg/L and 1.22 ± 0.75 mg/L, $P < 0.001$ and $P < 0.001$). Similarly, there was significantly elevated MCP-1 levels in patients with unstable plaques (467.13 ± 66.28 pg/mL) than stable plaque and NC groups (351.84 ± 81.89 pg/mL and 153.64 ± 49.79 pg/mL, $P < 0.001$ and $P < 0.001$) (Fig. 2).

ROC of calcium content, spectral curve slope and serum levels of Hs-CRP, MCP-1 in plaque groups

The generated area under the curve (AUC) of the calcium content in carotid plaque is 0.938 and assumed cut-off calcium content for discriminating stable and unstable plaque was 101.5, with sensitivity of 73.33% and specificity of 100%. The generated AUC of slope of spectral curve is 0.942 and assumed cut-off slope of spectral curve for differentiating stable from unstable plaque was 3.835, with sensitivity of 96.67% and specificity of 77.27%. In addition, the generated area AUC of serum Hs-CRP level is 1 and the Hs-CRP threshold cutoff was determined to be 7.14 mg/L, with associated sensitivity and specificity of 100% and 100%, respectively. The generated AUC of serum MCP-1 level is 0.901 and the MCP-1 threshold cutoff was determined to be 392.3 pg/mL, with associated sensitivity and specificity of 84% and 100%, respectively (Fig. 3).

Correlation analysis

The age, complete blood counts (leukocyte and monocyte), calcium content and slope of spectral curve were not significantly correlated with serum levels of Hs-CRP or MCP-1 in either the patients or control groups. No obvious correlation was shown between the calcium content, spectral curve slope and serum levels of Hs-CRP, MCP-1 in either the patients with unstable plaques or those with stable plaques.

Medication use and cerebrovascular events

During 1-year follow-up, none of significant differences were shown in medication use between these two carotid atherosclerosis groups except more lipid-lowering drugs use in unstable plaque group than stable plaque group ($P < 0.001$). Ischemic stroke occurred in 2 (2/17, 11.8%) patients with unstable plaques and 2 (2/25, 8%) in patients with stable plaques, in the absence of transient ischemic attack (TIA) or intracranial hemorrhage (Table 2).

Table 2
Medication use and cerebrovascular events during 1-year follow-up

Variable	Unstable plaque (n = 17)	Stable plaque (n = 25)	P value
≥ 1 antiplatelet agent	15/17	24/25	0.556
≥ 1 antihypertensive agent	7/17	7/25	0.508
≥ 1 lipid-lowering agent	16/17	10/25	< 0.001
≥ 1 glucose-lowering agent	3/17	4/25	> 0.999
≥ 1 anticoagulant agent	0	0	
Quitting smoking	0	0	
CEA/CAS	0	0	
Outcome	2/17	2/25	> 0.999
Ischemic stroke	0	0	
TIA	0	0	
Intracranial hemorrhage			
CEA: Carotid endarterectomy; CAS: carotid artery stenting; TIA: transient ischemic stroke			

Discussion

With the advances in imaging techniques and deeper understanding of vulnerable carotid plaques, the traditional concept of adopting the degree of luminal stenosis as the unique imaging marker for determining treatment option is challenged by accumulating evidence revealing that plaque composition also plays a role in ischemic stroke and thrombotic complications, irrespective of the degree of stenosis [16–18]. Currently, such parameters of plaque imaging as intraplaque haemorrhage, plaque volume, inflammation and intraplaque neovascularization, carotid plaque thickness, lipid-rich necrotic core and fibrous cap, surface morphology, etc are considered imaging biomarkers of vulnerable carotid plaques [19]. Beyond these, more recently increasing data has demonstrated that atherosclerotic plaque calcification is a complex, active biological process involving in plaque vulnerability to rupture,

consequently leading to major cardiovascular events such as myocardial infarction [20, 21]. Clinical imaging modalities including non-invasive (e.g. CT) or invasive (e.g., intravascular ultrasound (IVUS), Optical coherence tomography (OCT)) methods, are utilized in description of calcified carotid plaque [21]. Inheriting the detection sensitivity of CT to calcium, GSI uses X-rays and expresses the absorption of the energy spectrum based on tissue composition and lesions, performing quantitative analysis via the material decomposition technique, of which the calcium map displays only calcium density and enable measurement of calcium content in plaque [22]. In the present study, patients with unstable plaques showed a decrease in calcium content compared with calcified plaques group. Together with the previous study suggesting less calcification associated with clinically symptomatic plaques rather than the asymptomatic ones [23], this finding indicates that GSI calcium content could be associated with plaque instability. Interestingly, our study also found that the spectral curve slope of CT value of plaque in the patients with stable plaques was significantly lower than the patients with unstable plaques, which is in parallel with a previous study reported by Karçaaltıncaba M,et al. that vulnerable plaques were rich in lipid cores, and their energy spectrum curve demonstrated a bow-up curve with a positive slope, while in contrast, stable plaques presented with a bow-down curve with a negative slope [24]. Of note, our further ROC curves analysis revealed the optimal diagnostic threshold values of calcium content and spectral curve slope to differentiate vulnerable plaque from stable plaque, as well as their distinctive specificity and sensitivity. Taken together, our results indicate that these two parameters could serve as a potential imaging biomarker relevant to plaque vulnerability or disease progression.

As the most promising indicator for vascular inflammation, CRP is one of the acute-phase proteins mainly produced in the liver during episodes of acute inflammation or infection. The Hs-CRP assay methods have been routinely adopted to detect small changes in CRP concentrations. Hs-CRP is nowadays considered a predictor of future cardiovascular events [25], and classified as Class III B level of evidence in 2016 European Guidelines on cardiovascular disease prevention [26], albeit still some remaining debates [27]. Various studies have provided strong evidence that CRP inhibits endothelial nitric oxide production [28] and contributes to plaque instability by activating nuclear factor κappa B (NF-κB) [29, 30], inducing the expression of MMP-1, -2, and − 9 [31, 32]. In line with these previous studies, our study showed that compared with either stable plaque or control group, patients with unstable plaques had remarkably elevated serum Hs-CRP levels and more strikingly, an optimal diagnostic threshold values were also obtained for separating vulnerable plaque from stable plaque with higher specificity and sensitivity than either calcium content or spectral curve slope, supporting the view that the derangement of this inflammatory biomarker is closely associated with the formation or development of vulnerable carotid plaques. This is noteworthy since a latest new strategy of multiplying individual profiles has been proposed by Nederkoorn, et al. for selection of patients with the highest risk and for the best treatment [33]. For instance, along with the Reynolds risk score, the addition of Hs-CRP as well as family history and traditional risk factors is reported to efficiently improve overall future risk prediction of cardiovascular events [34]. Nevertheless, more efforts are needed to address these issues in future research.

As a key chemokine, MCP-1 has been demonstrated to play important roles in atherosclerosis by promoting migration and infiltration of monocytes into the plaque through its receptor C-C chemokine

receptor 2 (CCR2) [35]. So far, limited data is available concerning the roles of MCP-1 in vulnerable carotid plaques [36]. Intriguingly, in an in vivo animal study on apolipoprotein E (ApoE)-/- mice, site-specific delivery of adenoviral-mediated shRNA targeting mouse MCP-1 downregulated MCP-1 expression, turned a vulnerable plaque into a more stable plaque phenotype and prevented plaque disruption, implicating its detrimental effects on plaque stability [37]. In parallel with these findings, it was found from this study that patients with unstable plaque had higher serum MCP-1 levels than either stable plaque or control group. Together with the ROC analysis results similar to that of calcium content or spectral curve slope, our findings strongly suggest that MCP-1 may potentially be involved in carotid plaque instability and hence utilized for assessment of plaques vulnerability [38].

In 1-year follow-up, no significant differences were shown in the occurrence of ischemic stroke between the unstable plaque group and stable plaque group, probably due to the better compliance and persistence of taking lipid-lowering drugs in the former group. We did not further investigate the relationship between these two GSI parameters and risk of ischemic stroke, largely because the sample size is too small to reach statistical significance.

In conclusion, this study shows marked alternation in GSI calcium content and spectral curve slope in patients with unstable plaques, reflecting a close link between calcification and plaque instability. More strikingly, these two imaging parameters have powerful diagnostic value in determination of unstable plaque with different threshold values, indicating that they could serve as valuable biomarkers related to atherosclerosis and plaque vulnerability in clinical practice. On the other hand, the small sample size is a major limitation of this study, and more sophisticated, larger-scale comparisons with histopathological specimens is also needed to validate the reliability of GSI-based CT carotid plaque imaging in the future. Moreover, this study also demonstrates altered serum levels of Hs-CRP and MCP-1 protein in patients with unstable plaques as well as their optimal diagnostic threshold values for determining unstable plaque, supporting the viewpoint that these pro-inflammatory molecules might be implicated in the process of plaque instability and hence utilized as serological biomarkers potentially predictive of vulnerable carotid plaques. In a word, our pilot study strongly supports the feasibility of using these serological and imaging parameters as multiple potential biomarkers relevant to plaque vulnerability or stroke progression. Nevertheless, our novel discoveries in GSI calcium content and the spectral curve slope in vulnerable carotid plaques certainly pave the way for identifying valuable candidate biomarkers in atherothrombotic stroke and more importantly, exploration of a new therapeutic strategy for effective stroke prevention.

Methods

Patients and controls

Forty-two patients with asymptomatic carotid atherosclerosis (27 men and 15 women; mean age 63.6 ± 10.4 years) were enrolled in this study. The research protocol was reviewed and approved by the Ethics Committee of Beijing Anzhen Hospital. All diagnostic procedures were performed in accordance with

relevant guidelines and regulations, and written informed consent from all study participants was obtained. All patients were diagnosed on the basis of medical history, clinical examination and results of brain MRI and MRA scans. Carotid duplex sonography was undertaken in all patients, who were further subdivided into stable plaque and unstable plaque groups in terms of plaques echolucency using carotid ultrasound with integrated backscatter (IBS). Nineteen healthy subjects (10 men and 9 women; mean age 60.3 ± 11.8 years) were included as normal controls (NC) without any evidence of carotid atherosclerosis, clinical history of cardiovascular and cerebrovascular events.

None of the participating individuals had (1) history of taking anti-platelets agent or statins; (2) autoimmune, hepatic, renal or cancerous diseases; (3) history of heart disease (such as atrial fibrillation, heart failure, acute coronary syndrome, rheumatic heart disease, dilated cardiomyopathy); or (4) a certified infection. The following diagnostic tests were performed in both patients and normal controls: complete blood counts, blood chemistry, Hs-CRP, electrocardiogram (EKG), posterior-anterior chest radiography, transthoracic cardiac echocardiography, transcranial Doppler ultrasonography and carotid duplex sonography.

Sample collection

All the whole blood samples were drawn between 09:00am and 12:00am. After brief centrifugation at 3000 rpm for 5 min, serum was collected and stored at − 70°C in small aliquots for further use.

CT protocols

After an injection of nonionic contrast agent (iopamidol,Bracco, Milan, Italy), GSI-CTA was performed with scan delay of 5 s using a 64-slice spiral CT scanner with a gemstone detector (GE Discovery CT 750 HD, GE Healthcare, Milwaukee, WI, USA). The flow rates and volume of contrast material were determined based on a fixed duration (12 seconds) of injection and dose tailored to the weight of each patient (252 mgI/kg). 65 ml of iopamidol (30 gI/100 ml) was intravenously injected at flow rate of 3.5 ml/s, followed by a 30 ml saline chaser at the same flow rate. Scanning was carried out in 0.6*0.625 mm GSI mode. The scanning parameters in the GSI mode were employed as following: tube voltage of 80/140 kV and 0.5-ms instantaneous switch; tube current, 600 mA; slice thickness, 0.625 mm; rotation speed, 0.8 s; helical pitch, 1.375 and matrix, 512 × 512.

Image evaluation

After scanning, The GSI viewer 4.5 (GE Healthcare, Milwaukee, WI, USA) was utilized for the further analysis. GSI plaque imaging was initially quantified for the carotid atherosclerotic plaque characterization. Briefly, the middle part of the ascending aorta was selected as the region of interest (ROI) where a threshold value of 100 HU was established. The minimum ROI volume was set on the plaque through the post processing technics, and characteristic spectral attenuation curve (HU) of the corresponding region was acquired. The points on the curve represent the average CT values of tissues at different keV levels. ROI is then placed in fat tissue, muscle fiber tissue and bone structure, respectively and as a consequence, three distinctive attenuation curves with different colors were obtained to

determine the nature of plaques (Fig. 1). Three categories of calcified or noncalcified plaques (NCP) were defined according to the average CT values: lipid cores plaques (unstable plaque), NCP < 30 HU; fibrous plaques (unstable plaque), 30 HU < NCP < 150 HU; calcified plaques (stable plaque), > 220 HU [14].

After qualitative analysis of atherosclerotic plaques, material decomposition (MD) analysis was chosen for measurement of intraplaque calcium content. Briefly, the energy range was set at 65 kev, followed by placing of the minimum ROI volume on the target plaque, ensuring that ROI was placed on the images with the original scanning layer thickness, particularly those with relatively uniform density, so as to detect the tissue content (g/L) of corresponding intraplaque structure. Calcium (water)-based material decomposition analysis was conducted as described elsewhere to measure intraplaque calcium content in the selected ROI area using extracted calcium map [15]. Additionally, the slope of spectral curve with context to the CT value of plaque was calculated, i.e., the difference between the CT values of two measured points on the energy spectrum curve was divided by the energy difference between these two points. In this study, since the single-energy CT values at 40kev and 110kev were selected as reference points, respectively, the value of the slope K of spectrum curve = (CTa -CTb)/70.

Immunoturbidimetry

Serum MCP-1 levels were measured by a commercial Immunoturbidimetry according to the supplier's directions (Boster Biological Technology co.ltd, USA) with a detection limit of 15.6 pg/ml. All assays were undertaken simultaneously in a blinded way.

1-year Follow-up

Trained investigators collected patients' data through telephone or face-to-face interviews at 1, 3, and 12 months after baseline measurements. Clinical events and medical therapy were evaluated at each follow-up visit among all patients. The primary outcome measures were a composite of stroke (either ischemic or hemorrhagic), or TIA, whichever occurred first. All of the primary outcome events and medical therapy were reviewed by two of the investigators.

Statistics

The quantitative data are presented as mean ± standard deviation (calcium content, Hs-CRP and MCP-1 levels) or median with range (spectral curve slope). The normal distributed data were processed using one-way analysis of variance (ANOVA) and Student–Newman–Keul's post-hoc test and Pearson's correlation test. Nonnormal distributed data were analyzed with Kruskal-Wallis ANOVA Spearman's correlation test. Chi-square test was used to compare the differences in the qualitative data (sex, diabetes, coronary artery disease, dyslipidemia, hypertension, smoking, peripheral artery disease, carotid stenosis) between groups. Receiver operating characteristic (ROC) curves were also analyzed for quantitative slope of spectral curve and calcium content, and areas under the ROC were calculated. $P < 0.05$ was deemed statistically significant.

Declarations

Ethical approval and consent to participate

All procedures performed in research involving human participants comply with the ethical standards of the institution and/or the National Research Council, and comply with the 1964 Declaration of Helsinki and its subsequent amendments or similar ethical standards. According to the Declaration of Helsinki, the study was approved by the Ethics Committee of Beijing Anzhen Hospital. All participants have obtained written informed consent.

Acknowledgements

We are grateful to Dr Li Wang for her instruction in gemstone spectral imaging. This work was supported by a grant from National Natural Science Foundation (NSF 82071342).

Author contributions

Guang-Zhi Liu and Li Wang conceived the experiment(s), Ze-Xin Fan, Xiao-Qing Li, Ting-Ting Yang and Kai Sun conducted the experiment(s), Shao-Jie Yuan, Tian-Tong Niu and Lin Ma analysed the results. All authors reviewed the manuscript.

Conflicts of interest

The authors declare that there are no conflicts of interest.

References

1. Bentzon, J. F., Otsuka, F., Virmani, R. & Falk, E. Mechanisms of plaque formation and rupture. Circ Res. 2014 Jun 6;114(12):1852-66. doi: 10.1161/CIRCRESAHA.114.302721.
2. Wolf, D. & Ley, K. Immunity and Inflammation in Atherosclerosis.Circ Res. 2019 Jan18;124(2):315–327. doi: 10.1161/CIRCRESAHA.118.313591.
3. Bäck, M., Yurdagul, A. Jr, Tabas, I., Öörni, K. & Kovanen, P. T. Inflammation and its resolution in atherosclerosis: mediators and therapeutic opportunities. *Nat Rev Cardiol.* **16** (7), 389–406 https://doi.org/10.1038/s41569-019-0169-2 (2019 Jul).
4. Zhao, H. *et al.* Association of carotid atherosclerotic plaque features with acute ischemic stroke: a magnetic resonance imaging study. *Eur J Radiol.* **82** (9), e465–70 https://doi.org/10.1016/j.ejrad.2013.04.014 (2013 Sep).
5. Gupta, A. *et al.* Carotid plaque MRI and stroke risk: a systematic review and meta-analysis. *Stroke.* **44** (11), 3071–3077 https://doi.org/10.1161/STROKEAHA.113.002551 (2013 Nov).

6. Fisher, M., Blumenfeld, A. M. & Smith, T. W. The importance of carotid artery plaque disruption and hemorrhage. *Arch Neurol.* **44** (10), 1086–1089 https://doi.org/10.1001/archneur.1987.00520220082022 (1987 Oct).
7. Stary, H. C. *et al.* A definition of advanced types of atherosclerotic lesions and a histological classification of atherosclerosis. A report from the Committee on Vascular Lesions of the Council on Arteriosclerosis, American Heart Association. Circulation. 1995 Sep 1;92(5):1355-74. doi: 10.1161/01.cir.92.5.1355.
8. Gao, T., Zhang, Z., Yu, W., Zhang, Z. & Wang, Y. Atherosclerotic carotid vulnerable plaque and subsequent stroke: a high-resolution MRI study. *Cerebrovasc Dis.* **27** (4), 345–352 https://doi.org/10.1159/000202011 (2009).
9. Lusis, A. J. & Atherosclerosis Nature. 2000 Sep 14;407(6801):233 – 41. doi: 10.1038/35025203.
10. Takaya, N. *et al.* Association between carotid plaque characteristics and subsequent ischemic cerebrovascular events: a prospective assessment with MRI–initial results.Stroke. 2006Mar;37(3):818–23. doi: 10.1161/01.STR.0000204638.91099.91.
11. Murgia, A. *et al.* Plaque imaging volume analysis: technique and application. Cardiovasc Diagn Ther. 2020 Aug;10(4):1032–1047. doi: 10.21037/cdt.2020.03.01.
12. Lorsakul, A. *et al.* Numerical observer for atherosclerotic plaque classification in spectral computed tomography. *J Med Imaging (Bellingham).* **3** (3), 035501 https://doi.org/10.1117/1.JMI.3.3.035501 (2016 Jul).
13. Shinohara, Y. *et al.* Carotid Plaque Evaluation Using Gemstone Spectral Imaging: Comparison with Magnetic Resonance Angiography. *J Stroke Cerebrovasc Dis.* **26** (7), 1535–1540 https://doi.org/10.1016/j.jstrokecerebrovasdis.2017.02.036 (2017 Jul).
14. Motoyama, S. *et al.* Multislice computed tomographic characteristics of coronary lesions in acute coronary syndromes. J Am Coll Cardiol. 2007 Jul 24;50(4):319 – 26. doi: 10.1016/j.jacc.2007.03.044.
15. Yue, D. *et al.* The relationship between calcium (water) density and age distribution in adult women with spectral CT: initial result compared to bone mineral density by dual-energy X-ray absorptiometry. *Acta Radiol.* **60** (6), 762–768 https://doi.org/10.1177/0284185118801139 (2019 Jun).
16. Millon, A. *et al.* High-resolution magnetic resonance imaging of carotid atherosclerosis identifies vulnerable carotid plaques. *J Vasc Surg.* **57** (4), 1046–10512 https://doi.org/10.1016/j.jvs.2012.10.088 (2013 Apr).
17. Grimm, J. M. *et al.* Comparison of symptomatic and asymptomatic atherosclerotic carotid plaques using parallel imaging and 3 T black-blood in vivo CMR. J Cardiovasc Magn Reson. 2013 May 24;15(1):44. doi: 10.1186/1532-429X-15-44.
18. Yamada, K. *et al.* High-Intensity Signal in Carotid Plaque on Routine 3D-TOF-MRA Is a Risk Factor of Ischemic Stroke. *Cerebrovasc Dis.* **41** (1–2), 13–18 https://doi.org/10.1159/000441094 (2016).
19. Saba, L. *et al.* Imaging biomarkers of vulnerable carotid plaques for stroke risk prediction and their potential clinical implications. *Lancet Neurol.* **18** (6), 559–572 https://doi.org/10.1016/S1474-

4422(19)30035-3 (2019 Jun).

20. Bailey, G., Meadows, J. & Morrison, A. R. Imaging Atherosclerotic Plaque Calcification: Translating Biology. *Curr Atheroscler Rep.* **18** (8), 51 https://doi.org/10.1007/s11883-016-0601-6 (2016 Aug).
21. Barrett, H. E., Van der Heiden, K., Farrell, E., Gijsen, F. J. H. & Akyildiz, A. C. Calcifications in atherosclerotic plaques and impact on plaque biomechanics.J Biomech. 2019 Apr18;87:1–12. doi: 10.1016/j.jbiomech.2019.03.005.
22. Wintermark, M. *et al.* High-resolution CT imaging of carotid artery atherosclerotic plaques. *AJNR Am J Neuroradiol.* **29** (5), 875–882 https://doi.org/10.3174/ajnr.A0950 (2008 May).
23. Kwee, R. M. Systematic review on the association between calcification in carotid plaques and clinical ischemic symptoms. *J Vasc Surg.* **51** (4), 1015–1025 https://doi.org/10.1016/j.jvs.2009.08.072 (2010 Apr).
24. Karçaaltıncaba, M. & Aktaş, A. Dual-energy CT revisited with multidetector CT: review of principles and clinical applications. *Diagn Interv Radiol.* **17** (3), 181–194 https://doi.org/10.4261/1305-3825.DIR.3860-10.0 (2011 Sep).
25. Emerging Risk Factors Collaboration *et al.* C-reactive protein, fibrinogen, and cardiovascular disease prediction. *N Engl J Med.* **4** (14), 1310–1320 https://doi.org/10.1056/NEJMoa1107477 (2012 Oct).
26. Piepoli, M. F. *et al.* 2016 European Guidelines on cardiovascular disease prevention in clinical practice. Eur Heart J. 2016 Aug 1;37(29):2315–2381. doi: 10.1093/eurheartj/ehw106.
27. Yousuf, O. *et al.* High-sensitivity C-reactive protein and cardiovascular disease: a resolute belief or an elusive link? *J Am Coll Cardiol.* **30** (5), 397–408 https://doi.org/10.1016/j.jacc.2013.05.016 (2013 Jul).
28. Guan, H. *et al.* Adeno-associated virus-mediated human C-reactive protein gene delivery causes endothelial dysfunction and hypertension in rats. *Clin Chem.* **55** (2), 274–284 https://doi.org/10.1373/clinchem.2008.115857 (2009 Feb).
29. Hattori, Y., Matsumura, M. & Kasai, K. Vascular smooth muscle cell activation by C-reactive protein. Cardiovasc Res. 2003 Apr 1;58(1):186 – 95. doi: 10.1016/s0008-6363(02)00855-6.
30. Kawanami, D. *et al.* C-reactive protein induces VCAM-1 gene expression through NF-kappaB activation in vascular endothelial cells. *Atherosclerosis.* **185** (1), 39–46 https://doi.org/10.1016/j.atherosclerosis.2005.01.057 (2006 Mar).
31. Cimmino, G. *et al.* C-reactive protein induces expression of matrix metalloproteinase-9: a possible link between inflammation and plaque rupture. Int J Cardiol. 2013 Sep 30;168(2):981-6. doi: 10.1016/j.ijcard.2012.10.040.
32. Doronzo, G., Russo, I., Mattiello, L., Trovati, M. & Anfossi, G. C-reactive protein increases matrix metalloproteinase-2 expression and activity in cultured human vascular smooth muscle cells. *J Lab Clin Med.* **146** (5), 287–298 https://doi.org/10.1016/j.lab.2005.07.010 (2005 Nov).
33. Nederkoorn, P. J. Vulnerable carotid plaque and biomarkers: multiplying individual risk profiles? *Eur J Neurol.* **26** (12), 1425 https://doi.org/10.1111/ene.14064 (2019 Dec).

34. Ridker, P. M., Buring, J. E., Rifai, N. & Cook, N. R. Development and validation of improved algorithms for the assessment of global cardiovascular risk in women: the Reynolds Risk Score. *JAMA.* **14** (6), 611–619 https://doi.org/10.1001/jama.297.6.611 (2007 Feb).
35. Moriya, J. Critical roles of inflammation in atherosclerosis. *J Cardiol.* **73** (1), 22–27 https://doi.org/10.1016/j.jjcc.2018.05.010 (2019 Jan).
36. Wahlgren, C. M., Zheng, W., Shaalan, W., Tang, J. & Bassiouny, H. S. Human carotid plaque calcification and vulnerability. Relationship between degree of plaque calcification, fibrous cap inflammatory gene expression and symptomatology. *Cerebrovasc Dis.* **27** (2), 193–200 https://doi.org/10.1159/000189204 (2009).
37. VanGilder, R. L. *et al.* C-reactive protein and long-term ischemic stroke prognosis. *J Clin Neurosci.* **21** (4), 547–553 https://doi.org/10.1016/j.jocn.2013.06.015 (2014 Apr).
38. Liu, X. L. *et al.* Local gene silencing of monocyte chemoattractant protein-1 prevents vulnerable plaque disruption in apolipoprotein E-knockout mice. *PLoS One.* **7** (3), e33497 https://doi.org/10.1371/journal.pone.0033497 (2012).

Figures

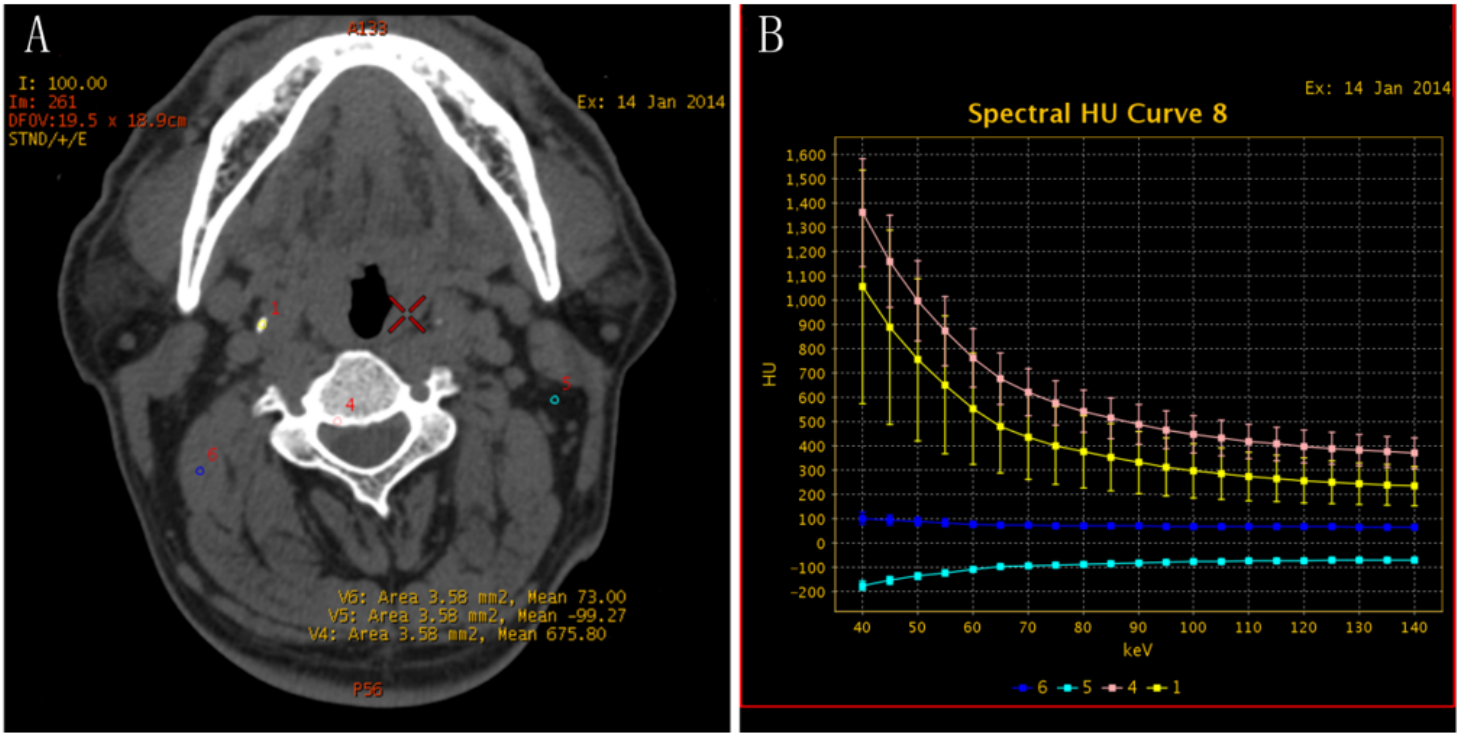

Figure 1

Gemstone spectral imaging (GSI) of carotid plaque. On the source images, ROI was placed on plaque, bone, muscle and fat, in order to obtain the spectrum curve (A). As the indicator of different tissue structure, pink, yellow, blue and green represent bone, plaque, muscle and fat, respectively. The plaque was judged as stable plaque, because its curve similarity to that of bone structure, and the corresponding

CT value more than 220 HU (B). The slope of spectral curve with context to the CT value of plaque was calculated, i.e., the difference between the CT values of two measured points on the energy spectrum curve was divided by the energy difference between these two points. In this study, since the single-energy CT values at 40kev and 110kev were selected as reference points, respectively, the value of the slope K of spectrum curve = (CTa -CTb)/70. ROI, regions of interest.

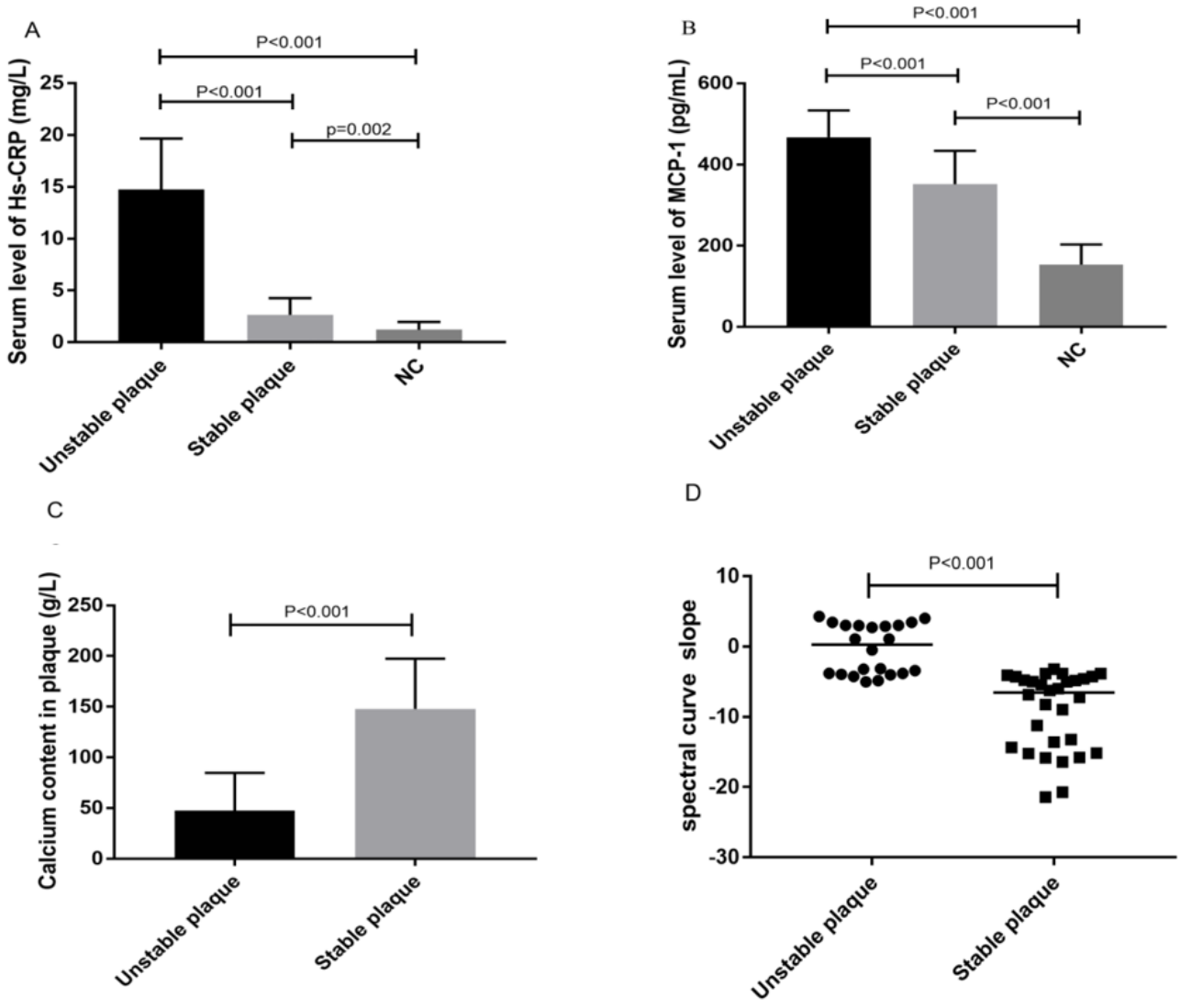

Figure 2

Serum level of high-sensitivity C-reactive protein (Hs-CRP), monocyte chemotactic protein-1 (MCP-1) in the three groups, spectral curve slope and calcium content in the plaque groups. Serum levels of Hs-CRP (A), MCP-1 (B) are compared between patients with stable plaques, unstable plaques and normal controls (NC) using an immunoturbidimetry. Calcium contents in plaque (C) and spectral curve slope of plaque (D) are compared between patients with stable plaques and unstable plaques using a gemstone spectral imaging (GSI). Horizontal lines indicate mean values with standard deviation or median values, numerals on top are p-values.

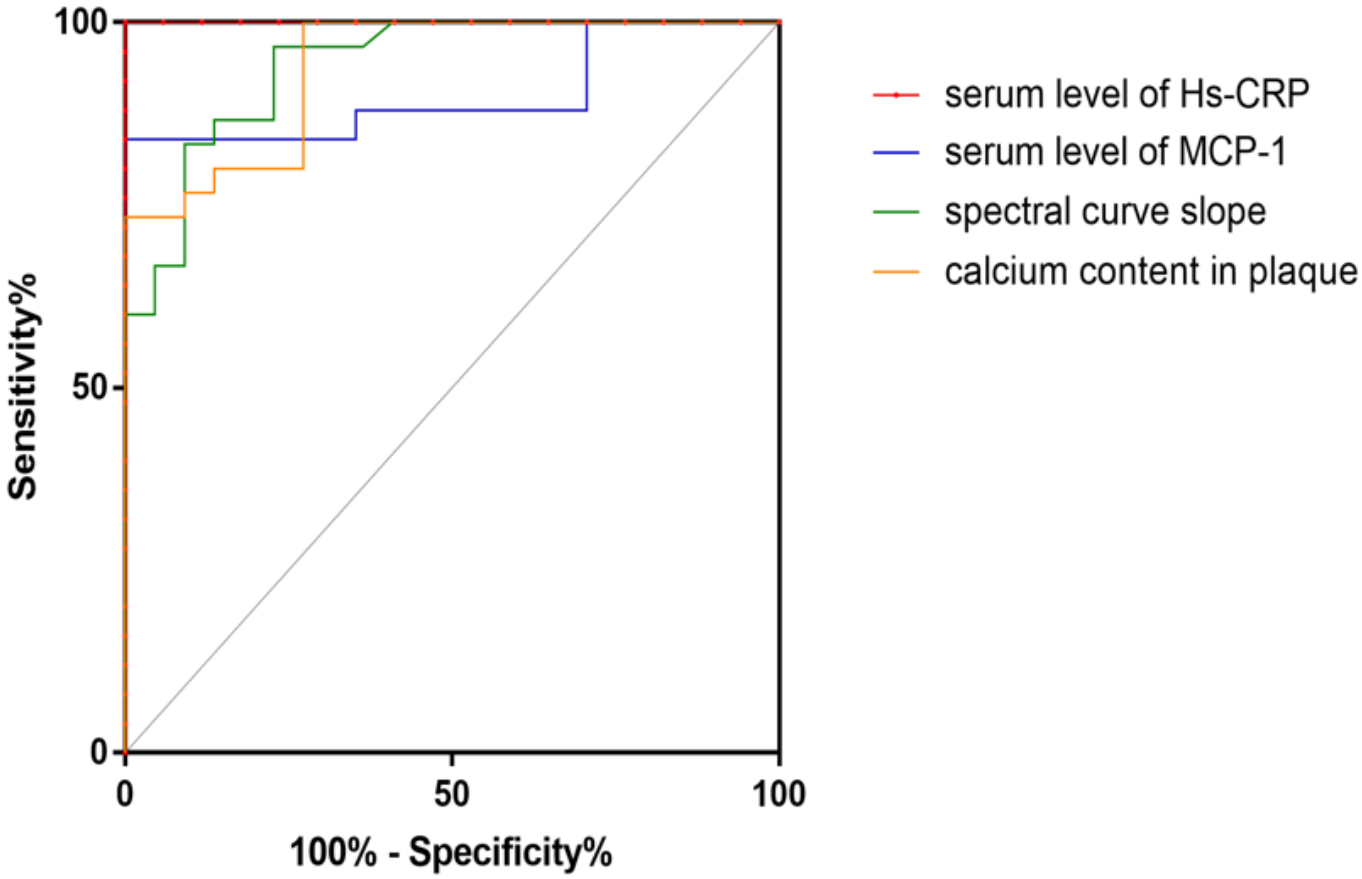

Figure 3

Receiver operating characteristic (ROC) of spectral curve slope, calcium content in plaque, serum levels of Hs-CRP, MCP-1 in plaque groups. Quantitative analysis for curve slope of plaque (green line), calcium content in plaque (orange line), serum MCP-1 level (blue line) and serum Hs-CRP level (red line) in plaque groups was performed using ROC curve analysis. The generated area AUC of the calcium content in plaque is 0.938 and assumed cut-off calcium content for discriminating stable and unstable plaque was 101.5 (g/L), with sensitivity of 73.33% and specificity of 100%. The generated AUC of slope of spectral curve is 0.942 and assumed cut-off slope of spectral curve for differentiating stable from unstable plaque was 3.835, with sensitivity of 96.67% and specificity of 77.27%. The generated area AUC of serum Hs-CRP level is 1 and the Hs-CRP threshold cutoff was determined to be 7.14 mg/L, with associated sensitivity and specificity of 100% and 100%, respectively. The generated AUC of serum MCP-1 level is 0.901 and the MCP-1 threshold cutoff was determined to be 392.3 pg/mL, with associated sensitivity and specificity of 84% and 100%, respectively. ROC, receiver operating characteristic; AUC, area under the curve.

Supplementary Files

This is a list of supplementary files associated with this preprint. Click to download.

- SupplementalData.pdf